Size and Discretization Effects in Simulations of Coronary Hemodynamics

M. Neumann, F. Neumann, R. Karch, W. Schreiner
Department of Medical Computer Sciences, Department of Cardiothoracic Surgery, Institute of Experimental Physics, University of Vienna, Spitalgasse 23, A-1090 Vienna, Austria E-Mail:mn@pap.univie.ac.at

Abstract

Using the method of constrained constructive optimization, we have generated a series of anatomically similar, realistically branching arterial vessel trees which feed the same perfusion area but differ in the number of arterial segments. In order to consistently parameterize vessels of different size, the elastic properties for the individual segments were derived from a simple model depending solely on vessel radii. Simulations of the hemodynamics of these trees were performed by means of an equivalent electric network model, in which each vessel segment was either regarded as a microcompartment and replaced by a single electric circuit; alternatively, segments were treated as electric transmission lines, for which a discretized solution of the telegraph equations is readily obtained. Since for very short segments both viewpoints are equivalent, this provides a means of studying discretization effects. The electric network model has been used to investigate some of the essential hemodynamical properties, such as signal propagation and pulsatile waveforms, for a series of arterial trees in which both the number of segments and the discretization of the continuum equations was varied systematically.

1   Introduction

Realistic computer simulations of coronary hemodynamics in a hierarchically branching network of elastic vessels is an extremely complex task which can only be tackled by introducing drastic simplifications. Apart from inherent difficulties, such as that blood is an inhomogeneous, non-Newtonian fluid, and that the vascular tree is not a passive but an active system which reacts spontaneously to changes in the physiological conditions, one of the fundamental practical limitations is given by the fact that

24   Simulations in Biomedicine IV

in any simulation only a finite number of vessel segments can be taken into account. The hemodynamics of vascular trees is usually modeled by means of a (non-linear) electric network (Milnor [1]), because a numerical solution of the full three-dimensional hydrodynamic equations for a system comprising more than a few bifurcations is not feasible at present. To assign sensible parameters to the individual elements is a separate problem, but one feature every model of the coronary circulation has to incorporate, is the interplay between pulsatile perfusion pressure and the periodic contraction of the myocardium: During systole, when the perfusion pressure reaches a maximum, the concomitant increase in intramyocardial pressure reduces the cross-section of most vessels, thereby increasing their hydrodynamic resistance. As a consequence, total coronary inflow is initially reduced and does not reach its peak value until the beginning of diastole. Intramyocardial pressure is a function of both time and space, rising approximately linearly with depth from very low values in the epicardial layers to the level of the instantaneous left ventricular pressure in the subendocardium (Heineman & Grayson [2]).

In order to study these phenomena by simulation, we are developing an algorithm that allows us to generate, on the computer, vascular trees which are not only compatible with physiological observations but also *geometrically realizable*. This means that no two vessels penetrate into each other, and that the exact geometrical positions of all vessel segments are known (Schreiner & Buxbaum [3]). At present, our model is not yet able to describe the entire coronary circulation but only the clinically more relevant arterial vessel tree. Also, the algorithm for generating the trees was, until recently, limited to two-dimensional perfusion areas. The generalization to three dimensions is under way (Karch *et al.* [4]). However, even with a two-dimensional model we are already able to address two important methodological questions:

- What is a sensible minimum size for these trees? We are now routinely studying trees of $O(10^4)$ segments, but the more detail we include in the structure, the more expensive are both the generation of the tree *and* the subsequent hemodynamical simulations.

- Is a network of microcompartments a sufficiently fine approximation? This model may be interpreted as a very coarse discretization of the telegraph equations, but replacing entire vessel segments between bifurcations by single electric elements obviously requires that segments may be considered infinitesimally short.

2 The model

2.1 Growing the trees

The method of "constrained constructive optimization" has been described in detail elsewhere (Schreiner & Buxbaum [3]). Briefly, the arterial tree is grown from an arbitrarily placed first segment by successively adding further segments which connect a randomly chosen point within the perfusion area to one of the existing segments. Both, the segment to which the connection is made and the position of the newly created bifurcation, are determined through an optimization procedure based on a target function of the form

$$T = \sum_j \ell_j r_j^\lambda \to \min, \qquad (1)$$

where ℓ_j and r_j are the length and (internal) radius of segment j, λ is a parameter, and the sum is over all segments created so far. (For $\lambda = 2$ the tree's total intravasal volume is being minimized.) At each bifurcation the radii of parent and left and right daughter segments are assumed to obey a "power law"

$$r_j^\gamma = r_{l(j)}^\gamma + r_{r(j)}^\gamma, \qquad (2)$$

with the exponent usually set to $\gamma = 3$ (Sherman [5]). An additional constraint requires that, given a certain pressure difference between the entrance and the terminal sites of the tree, the resulting net flow is the same for each step of the optimization procedure and is evenly distributed over all terminal sites. The hydrodynamic resistance is calculated assuming that all segments are straight cylindrical tubes and that Poiseuille's law is applicable. This determines the segments' internal radii, but how they are connected at bifurcations is not specified by the model.

For the present study, seven arterial trees, consisting of $N_{\text{term}} = 125, 250,$ ..., 8000 terminal segments (i.e. $N_{\text{tot}} = 2N_{\text{term}} - 1 = 249, 499, \ldots, 15999$ segments altogether), were generated in this way. The perfusion area was a circular disk of 5 cm radius, and perfusion pressure, terminal pressure, and total arterial blood flow were set to $p_{\text{perf}} = 100\,\text{mm Hg}$, $p_{\text{term}} = 60\,\text{mm Hg}$, and $Q_{\text{tot}} = 11.3\,\text{ml/s}$ (Schreiner & Buxbaum [3]). The topology and general appearance of the trees are governed by the characteristics of the random number generator, since the latter determines where, and in what order, perfusion sites are added. Therefore, all trees were grown from the same "seed". As can be seen from Fig. 1, they are "anatomically" and functionally very similar and differ only in "resolution", i.e. in the density of perfusion sites and in the number of bifurcations traversed by blood flowing from the root to one of the terminal sites. Any functional differences will therefore be due to the difference in size, rather than to anatomical differences.
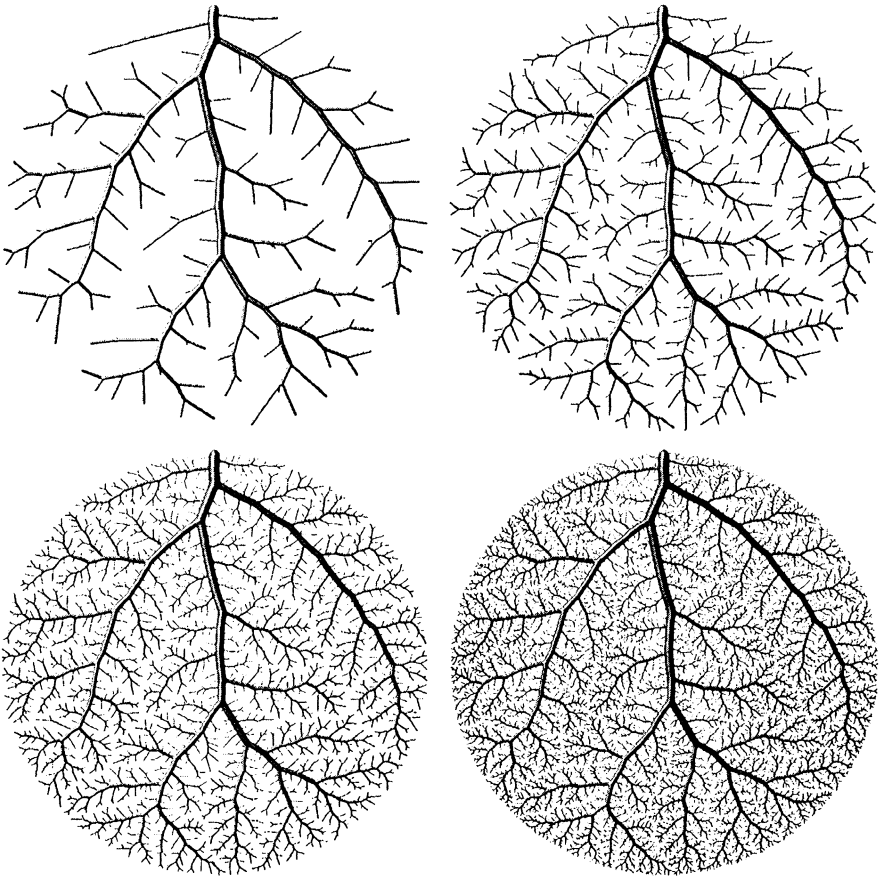
Figure 1: Anatomically similar arterial trees, grown from the same "seed" and feeding the same perfusion area, but differing in the number of terminal segments: $N_{\text{term}} = 125$, 500, 2000, and 8000.

2.2   Parameter assignment

The second important prerequisite for hemodynamical simulations is a pressure-radius relation. Although individual segments are modeled as straight cylindrical tubes whose length is given (and therefore fixed) by the positions of the bifurcations, their radii will vary with time, depending on the instantaneous values of internal and external (intramyocardial) pressure. This in turn determines a vessel's other properties, such as resistance to flow, compliance, etc.

   Despite the vast literature on elastic properties of a few selected blood vessels, we seem to know little or nothing about the dependence of these

properties on vessel size within a specific organ of a given individual. There-
fore, we have postulated a simple model allowing us to give at least a qual-
itative estimate of these properties for *all* segments of a vessel tree, i.e.
over a range of radii spanning almost two orders of magnitude (Neumann *et
al.* [6]). Assuming that radius r_0 and wall thickness h_0 of a relaxed segment
are correlated by a power law, $h_0 = ar_0^b$ (Podesser *et al.* [7]), that Laplace's
law for thin-walled tubes is applicable, that circumferential stress and strain
obey an exponential relationship, and that viscoelasticity may be ignored,
we obtain

$$\frac{(p_{\text{int}} - p_{\text{ext}})\, r}{\sqrt{r^2 + 2r_0 h_0 + h_0{}^2} - r} - p_{\text{ext}} =$$

$$\frac{E_0}{E_1} \left\{ \exp\left[E_1 \left(\frac{r + \sqrt{r^2 + 2r_0 h_0 + h_0{}^2}}{2r_0 + h_0} - 1 \right) \right] - 1 \right\}. \tag{3}$$

Here, r is the vessel radius at internal pressure p_{int} and intramyocardial
pressure p_{ext}, and the elastic parameters E_0 and E_1 are assumed to be the
same for all segments.

2.3   Electric network model

If the description of flow through a long elastic tube may be simplified by
assuming a flat velocity profile, the three-dimensional hydrodynamic equa-
tions are reduced to a one-dimensional form. If the latter can be linearized—
and this should be permissible, except for the aorta—a pair of equations for
internal pressure $p(x,t)$ and flow $Q(x,t)$ results, which is isomorphic to the
telegraph equations of electric transmission line theory (Milnor [1]):

$$\hat{L}\,\frac{\partial Q}{\partial t} = -\frac{\partial p}{\partial x} - \hat{R}\,Q\,, \tag{4}$$

$$\hat{C}\,\frac{\partial p}{\partial t} = -\frac{\partial Q}{\partial x}\,. \tag{5}$$

Here, $\hat{L} = \rho/r^2\pi$, $\hat{R} = 8\eta/r^4\pi$, and $\hat{C} = 2r\pi\partial r/\partial p$ denote inductance,
resistance, and capacitance (compliance) of the vessel per unit length, while
ρ and η are mass density and viscosity of blood.

In order to discretize Eqs. (4–5), each segment j of the arterial tree is
subdivided into a large number, $k_{\max}(j)$, of infinitesimal "slices", charac-
terized by a thickness $\ell_{j,k} = \ell_j/k_{\max}(j)$, inductance $L_{j,k} = \hat{L}\,\ell_{j,k}$, resistance
$R_{j,k} = \hat{R}\,\ell_{j,k}$, and capacitance $C_{j,k} = \hat{C}\,\ell_{j,k}$. Replacing the spatial deriva-
tives by forward differences leads to the following system of coupled ordinary
differential equations:

$$L_{j,k}\,\frac{\partial Q_{j,k}}{\partial t} = -\Big[(p_{\text{int}})_{j,k} - (p_{\text{int}})_{j,k-1} \Big] - R_{j,k}\,Q_{j,k}\,, \tag{6}$$

$$C_{j,k}\left[\left(\frac{\partial p_{\text{int}}}{\partial t}\right)_{j,k} + \left(\frac{\partial r/\partial p_{\text{ext}}}{\partial r/\partial p_{\text{int}}}\right)_{j,k}\left(\frac{\partial p_{\text{ext}}}{\partial t}\right)_{j,k}\right] = -\left[Q_{j,k+1} - Q_{j,k}\right]. \quad (7)$$

In the latter equation we have also taken into account that the rate of change of volume in slice k of segment j is not only a function of internal pressure but depends also explicitly on intramyocardial (external) pressure (Neumann *et al.* [6]). If $Q_{j,k}$ is interpreted as proximal flow into slice (j, k), and $(p_{\text{int}})_{j,k}$ as internal pressure at its distal end, then Eqs. (6–7) are equivalent to replacing segment j by a series of $k_{\max}(j)$ identical RLC-elements with pressure-dependent impedances $L_{j,k}$, $R_{j,k}$, and $C_{j,k}$. The junction conditions at bifurcations are continuity of pressure and conservation of flow.
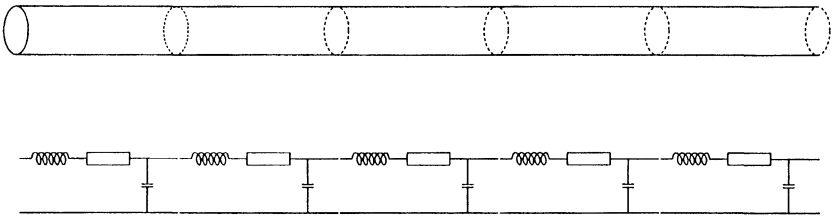

Figure 2: Discretization of transmission line equations.

As to the number of slices per segment, at the coarsest level of discretization we may try to replace an entire segment by a single RLC-element; on the other hand, the exact solution of the partial differential equations, Eqs. (4–5), is only obtained in the limit of infinitely small slices. How large a number is required in practice, will depend on the wavelength of the phenomena studied.

3   Results

3.1   Input impedances

Input impedances, defined as the ratio of (complex) perfusion pressure to total inflow, as a function of frequency ω, are often employed to characterize certain aspects of the systemic or pulmonary circulation (Milnor [1]). In the case of the coronary arteries, whose properties are continually changing due to the workings of the myocardium, this would not seem to be a very useful concept. However, if *differential* impedances are considered, i.e. the flow response to a weak, periodic pressure perturbation superimposed on a stationary reference state, these are actually quite valuable for quickly assessing the effects of various approximations—provided an appropriate range of reference states is probed.

As an example, we have calculated the input impedance, Z_{inp}, for the smallest and largest tree discussed in Sec. 2.1, for two typical reference

states: stationary flow between perfusion and terminal pressures of $p_{\text{perf}} = 100 \, \text{mm Hg}$ and $p_{\text{term}} = 60 \, \text{mm Hg}$, with the intramyocardial pressure either set to $p_{\text{ext}} = 0$ or $p_{\text{ext}} = 100 \, \text{mm Hg}$. In both cases the input impedance of the tree was calculated as the total impedance of the equivalent electric network, while the impedance of an individual segment was taken to be either that of a single RLC-element (coarsest discretization)

$$Z_j = R_j + i\omega L_j + \frac{Z_j^{(T)}}{1 + i\omega C_j Z_j^{(T)}}, \tag{8}$$

or that of a (continuous) transmission line (Milnor [1]),

$$Z_j = Z_j^{(0)} \frac{Z_j^{(T)} + Z_j^{(0)} + (Z_j^{(T)} - Z_j^{(0)}) \exp(-2i\omega C_j Z_j^{(0)})}{Z_j^{(T)} + Z_j^{(0)} - (Z_j^{(T)} - Z_j^{(0)}) \exp(-2i\omega C_j Z_j^{(0)})}. \tag{9}$$

Here, $Z_j^{(0)} = \sqrt{(R_j + i\omega L_j)/i\omega C_j}$ is the characteristic, and $Z_j^{(T)}$ the terminal (distal) impedance of segment j.

The results for the case that $Z_j^{(T)} = 0$ for all terminal segments (pressure reservoir at p_{term}) are displayed in Fig. 3. In order to show the differences more clearly, the plot extends up to 100 Hz, although a frequency range of 30–50 Hz is more than sufficient to describe pulsatile flow.
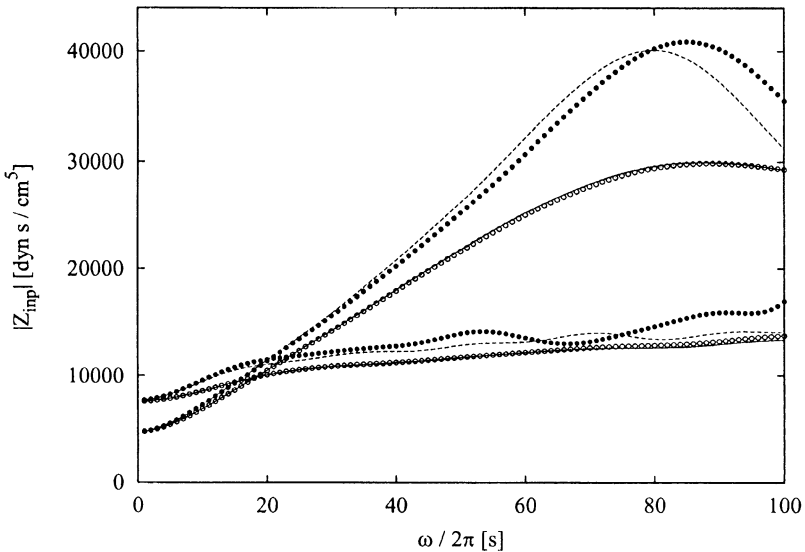

Figure 3: Modulus of differential input impedance for arterial trees under steady-state conditions. Upper (lower) set of curves: $p_{\text{ext}} = 0$ ($p_{\text{ext}} = 100 \, \text{mm Hg}$); dashed lines and full circles: $N_{\text{term}} = 125$; solid lines and open circles: $N_{\text{term}} = 8000$; lines (symbols): individual segments treated as continuous transmission lines (single RLC-elements).

It is immediately apparent that both the static value and the frequency behavior of Z_{inp} are strongly influenced by the intramyocardial pressure level. The curves also show a marked dependence on the size of the model tree, which is relatively more pronounced at the lower frequencies if the intramyocardial pressure is high enough. On the other hand, whether vessel segments are subdivided into one or more slices, seems to have no noticeable effect in the lower frequency range, so that the idea of treating each segment as a single RLC-element appears to be perfectly justified. Of course this is hardly surprising, since for our model the phase velocities are in the range of 5–15 m/s. Given a maximum frequency of about 30 Hz, the shortest wavelength is of the order of 20 cm, i.e. much larger than the length of an individual segment.

3.2   Signal propagation

Since input impedances are only a measure of the global properties of a system, the propagation of signals, being more sensitive to size and discretization effects, were investigated next. The trees were prepared in a static or stationary state at time $t = 0$, and the propagation of a pressure "wavelet"

$$\Delta p(t) = A \frac{t(2\tau - t)}{\tau^2} \sin\left(\frac{\pi t}{\tau}\right), \qquad 0 < t < 2\tau, \tag{10}$$

along the main path of the tree was studied. In Eq. (10), A is the amplitude of the perturbation superimposed on the perfusion pressure, and 2τ is the length of the wavelet. (The "main path" is the set of all segments traversed if one starts at the root and turns into the larger daughter segment at each bifurcation; for the trees considered here, it is 10–11 cm long.)

Figure 4 shows the propagation of a wavelet with $A = 5$ mm Hg and $\tau = 10$ ms, for trees prepared in a static state characterized by $p_{\text{ext}} = 0$ and $p_{\text{perf}} = p_{\text{term}} = 100$ mm Hg (so that $p_{\text{int}} = 100$ mm Hg everywhere and there is no net flow). The top part of the figure presents the time-course of the pressure signal at ten equidistant sites on the main path of the smallest ($N_{\text{term}} = 125$) tree, at the coarsest level of discretization. Both the propagation from left to right and the rapid decay of the pressure wave are clearly visible. At the center and bottom, we compare the signals measured at two selected sites, when either the size of the trees or the discretization level is being varied. As in the previous section, the size of the trees is seen to have a considerable influence, while a finer discretization produces hardly any effect—even for the tree with the fewest (i.e. longest) segments.
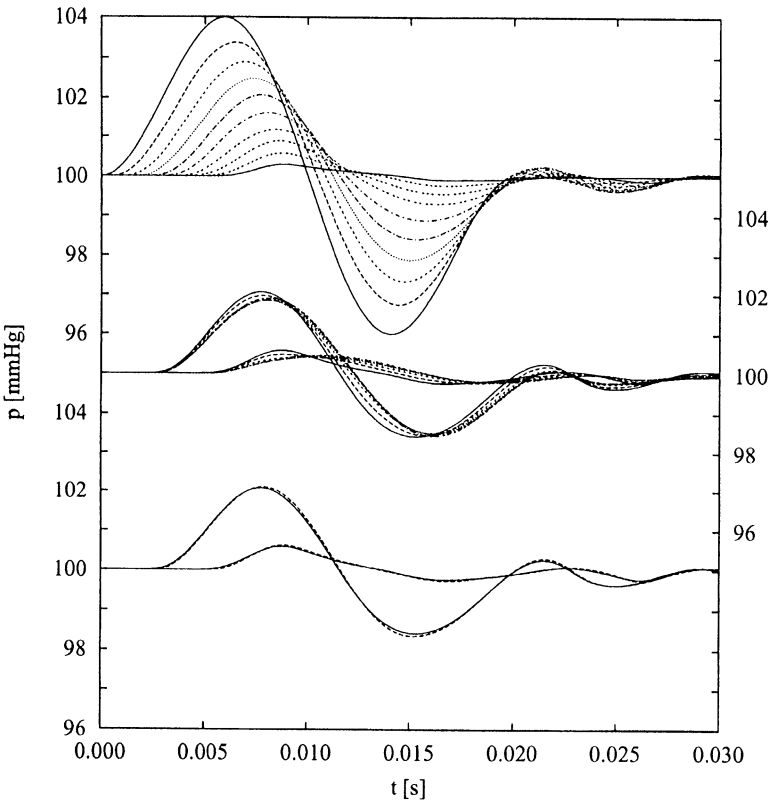
Figure 4: Propagation of pressure wavelet in arterial trees under static conditions. Top: pressure signals recorded every cm along the main path of a tree with $N_{\text{term}} = 125$ and segments modeled by single RLC-elements; center: comparison of signals at sites 4 and 8 cm from the entrance, obtained for trees varying in size between $N_{\text{term}} = 125$ and 8000; bottom: tree with $N_{\text{term}} = 125$ and segments modeled either by single RLC-elements (full lines) or transmission lines (dashed lines).

A more quantitative comparison is provided by Fig. 5, where the transit time t_{transit}, i.e. the time it takes a feature of the wavelet (in our case the point of half height before the first maximum) to travel a distance s down the main path, is plotted for trees subject to the same conditions as in Fig. 4. The upper part of Fig. 5, presenting the transit times for trees with 125 to 8000 terminal segments (treated as single RLC-elements), shows that trees with 1000–2000 or more terminal sites yield virtually equivalent results. Interestingly, the relationship between t_{transit} and s is approximately linear (except for the most distal part of the main path, which may be influenced by reflection at the terminal boundary conditions) and the signal propagation velocity inferred from the slope is about 17 m/s. The lower part

32   Simulations in Biomedicine IV

of Fig. 5 demonstrates once again that subdividing segments into slices has only negligible effects.

Signal propagation has also been studied for other, non-static conditions, and in particular for the flow wave, with similar results regarding size and discretization dependence.
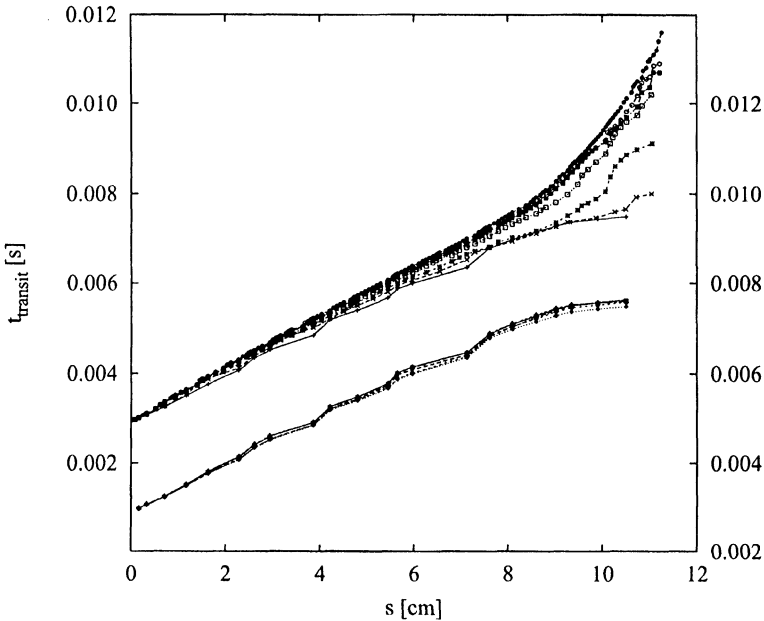

Figure 5: Transit time for a pressure wavelet traveling down the main path of arterial trees. Top: trees varying in size from $N_{\text{term}} = 125$ to 8000, with segments modeled as RLC-elements; bottom: tree with $N_{\text{term}} = 125$ and segments subdivided into increasingly finer slices, in order to approximate continuous transmission lines (shifted by -0.002 units for clarity).

3.3   Pulsatile flow

Our final test concerns the pulsatile flow along the main path, which results if the typical waveforms of aortic and left ventricular pressure—playing the part of perfusion and intramyocardial pressure, respectively—are applied to the model trees. Of course, the assumption that *all* segments are subject to the full left ventricular pressure, will overestimate the effect of intramyocardial "squeezing", but, with a two-dimensional model, any attempt to make the intramyocardial pressure inhomogeneous would be artificial. To be consistent with the optimization of the trees, all terminal segments were kept at a constant pressure of $p_{\text{term}} = 60 \, \text{mm Hg}$. This idea of representing

the microcirculation by a pressure reservoir is not very realistic either but should be irrelevant for the present purposes.
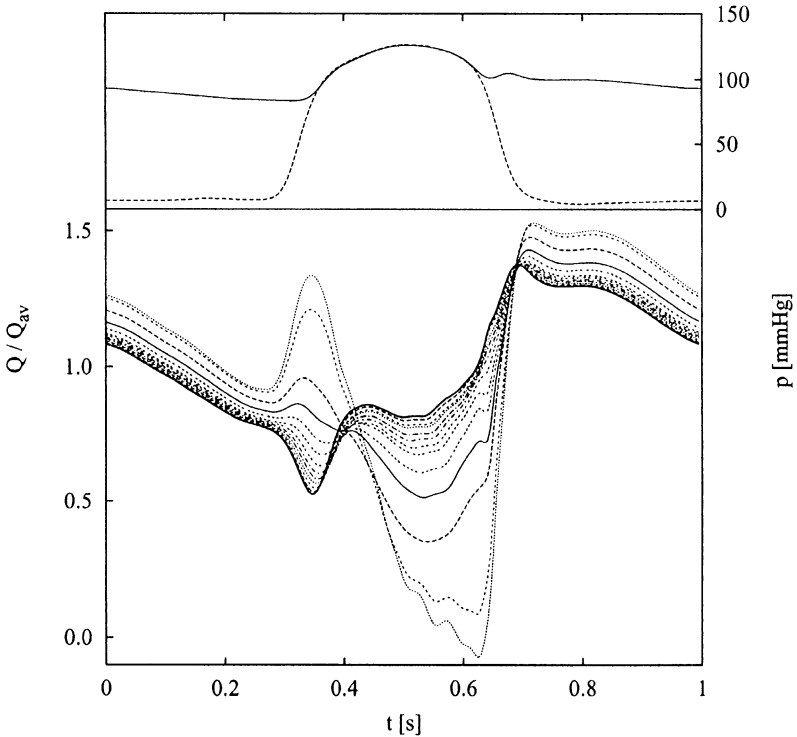

Figure 6: Pulsatile flow in an arterial tree with $N_{\text{term}} = 4000$ and segments modeled as single RLC-elements. Top: waveforms of aortic and left ventricular pressure; bottom: normalized flow at the entrance, every cm along its course, and at the terminal of the main path (from bottom to top at the far left and right).

Figure 6 shows the generic aortic and left ventricular waveforms (digitized from Milnor [1]) and, for a tree with 4000 terminals and no subdivision of segments, the resulting flow along the main path. (Since the flow decreases very rapidly with path-length, all curves have been normalized by the local time-averaged flow.) It is interesting to observe how, at the beginning of systole, the flow in the proximal part is initially reduced, while the distal segments are drained, and the pattern is reversed, before the flow in all segments reaches a maximum at the beginning of diastole.
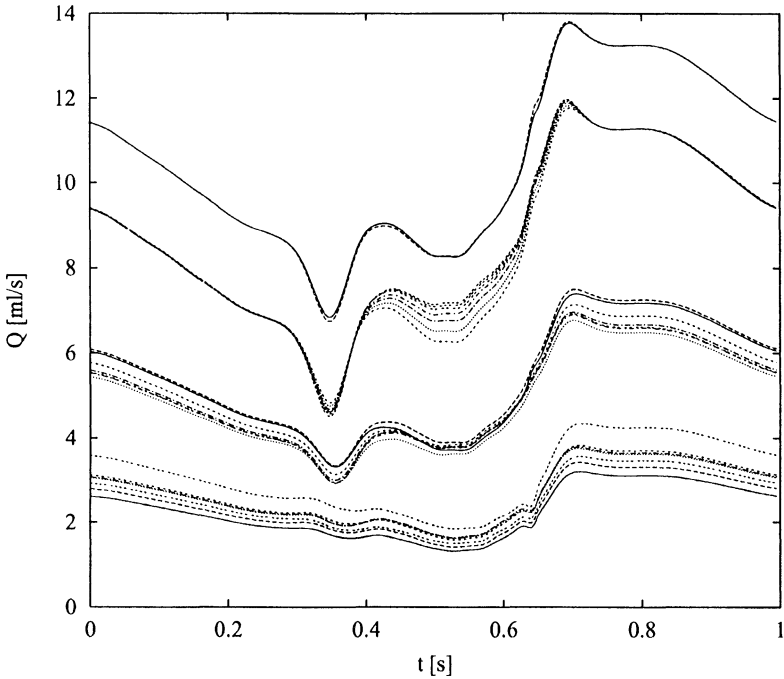
Figure 7: Pulsatile flow in arterial trees. Top: at the entrance of a tree with $N_{\text{term}} = 125$ and segments modeled as single RLC-elements (solid line) or transmission lines (dashed line); bottom three sets of curves: at the entrance and at two sites located 4, and 8 cm down the main path of trees with $N_{\text{term}} = 125, \ldots, 8000$ and no subdivision of segments. (For clarity, the topmost curve has been shifted by two units and the bottom two scaled by factors of 1.5 and 4, respectively.)

The topmost set of curves in Fig. 7 shows that even for a tree with only 125 terminal segments, subdividing the segments into slices has no significant effect on the total inflow. The lower part of the figure displays the dependence of the flow, measured at the entrance and two sites further down the main path, on the size (i.e. number of segments) of the tree. It is obvious that, at the entrance of the tree, the shape of the flow curve already shows a marked size-dependence, and this effect can only increase as one moves closer to the periphery of the tree. Nevertheless, we can say that, except very close to the periphery, the flow waveform is relatively well-defined for trees with $N_{\text{term}} \approx 2000$ or more terminal segments.

4   Conclusion

It has been shown for a detailed model of the arterial side of the coronary circulation, in which the blood supply to an unspecified microcirculatory network is effected by a series of anatomically similar vascular trees, that the model's hemodynamical behavior is largely independent of the size of the tree, if trees with 1000–2000 or more terminal segments are considered. In this case the individual vessel segments are also so short that they represent a sufficiently fine discretization of the underlying partial differential equations. In the present investigation unsteady flow has been modeled by means of the telegraph equations, but these conclusions may be expected to remain true if the one-dimensional hydrodynamic equations were used instead.

What has been studied here is merely the "convergence" of some hemodynamical properties with the spatial "resolution" of the model. It should be clear that other features of the model—e.g. vascular compliance; terminal boundary conditions; inhomogeneity of intramyocardial pressure; detailed hydrodynamical treatment; flow patterns near, and geometry of, bifurcations—may have a much larger influence.

References

1. Milnor, W.R. *Hemodynamics*, 2nd edition, Williams & Wilkins, Baltimore, 1989.

2. Heineman, F.W. & Grayson, J. Transmural distribution of intramyocardial pressure measured by micropipette technique, *American Journal of Physiology*, 1985, **249**, H1216–H1223.

3. Schreiner, W. & Buxbaum, P. Computer-optimization of vascular trees, *IEEE Transactions of Biomedical Engineering*, 1993, **40**, 482–491.

4. Karch, R., Schreiner, W., Neumann, F. & Neumann, M. Three-dimensional optimization of arterial tree models, this volume.

5. Sherman, T.F. On connecting large vessels to small: the meaning of Murray's law, *Journal of General Physiology*, 1981, **78**, 431–453.

6. Neumann, M., Neumann, F., Karch, R. & Schreiner, W. Spatially resolved simulation of coronary hemodynamics, in *Simulation Modelling in Bioengineering,* ed. M. Cerrolaza, D. Jugo & C.A. Brebbia, pp 39–51, Computational Mechanics Publications, Southampton, 1996.

7. Podesser, B., Neumann, F., Neumann, M., Schreiner, W., Wollenek, G. & Mallinger, R. Outer radius-wall thickness-ratio, a quantitative histology of the human coronary arteries, *Journal of Vascular Research*, submitted.